Articles

Au-Doped Magnetic Silica Nanotube for Binding of Cysteine-Containing Proteins

Doo Ri Bae,[†] Soo Jin Lee,[†] Sang Woo Han,[†] Jung Mi Lim,[‡] Dongmin Kang,[‡] and Jong Hwa Jung*,[†]

Department of Chemistry and Research Institute of Natural Science, Gyeongsang National University, Jinju 660-701, Korea, and Division of Life and Pharmaceutical Sciences, Ewha Womans University, 11-1 Daehyun-dong, Seodaemun-gu, Seoul 120-750, Korea

Received September 21, 2007. Revised Manuscript Received March 10, 2008

The Au-doped magnetic silica nanotube (**Au-MSNT**) was fabricated by sol−gel transcription and its binding ability for proteins was carried out by TEM, FT-IR, and confocal microscope. The nickel nanoparticles with 3.5 ± 1.0 nm are homogeneously deposited on the inner side of a silica nanotube (**SNT**) with 220 nm diameter. In addition, the **Au-MSNT** clearly revealed the Au nanoparticles with 9.3 ± 2.0 nm diameter. The **Au-MSNT** carried out the binding ability for protein as a guest molecule. The **Au-MSNT** acted as a receptor for the selective molecular recognition of biomolecules, particularly proteins containing cysteine. On the other hand, ubiquitin, which has no cysteine groups, was not immobilized onto the **Au-MSNT**. These results indicate that the **Au-MSNT** is efficiently recognized by the cysteine-containing protein.

Introduction

Magnetic particles such as superparamagnetic iron oxide and nickel particles have been extensively used for both in vitro and in vivo applications, such as magnetic resonance imaging (MRI) contrast enhancement, hyperthermia treatment, and gene and drug delivery.[1–4] In most applications, spherical nanoparticles have been used,[3] but they suffer from shortcomings related to control of particle sizes, surface functionalizations, and their environmental compatibility due to the structural limitations of spherical particles when multifunctionality is required on their surfaces.[5]

Since the recent demonstration of differential functionalization of silica nanotubes by Martin and co-workers[6] and Lee and co-workers,[5] nanoparticles with a tubular structure have been applied in the development of multifunctional nanoparticles. The structural attributes of nanotubes, such as the distinctive inner and outer surfaces, make them more attractive than the conventional spherical nanoparticles. The inner voids can be used for capturing,[6] concentrating,[7] and releasing species[7] ranging in size from large proteins to small molecules because tube dimensions can be easily controlled by the sol−gel template synthesis.[5a] The distinctive outer surfaces can be differentially functionalized with ecologically compatible ligands and/or probe molecules directed toward a specific target.[5,8] When the attractive tubular structure is combined with the magnetic property, the Au-doped magnetic silica nanotube (**Au-**

* Corresponding author. E-mail: jonghwa@gnu.ac.kr.
[†] Gyeongsang National University.
[‡] Ewha Womans University.

(1) For synthesis of magnetic nanoparticles, see: (a) Hyeon, T. *Chem. Commun.* **2003**, 927. (b) Sun, S.; Murray, C. B.; Weller, D.; Folks, L.; Moser, A. *Science* **2000**, *287*, 1989. (c) Grancharov, S. G.; Zeng, H.; Sun, S. H.; Wang, S. X.; O'Brien, S.; Murray, C. B.; Kirtley, J. R.; Held, G. A. *J. Phys. Chem. B* **2005**, *109*, 13030. (d) Redl, F. X.; Black, C. T.; Papaefthymiou, G. C.; Sandstrom, R. L.; Yin, M.; Zeng, H.; Murray, C. B.; O'Brien, S. P. *J. Am. Chem. Soc.* **2004**, *126*, 14583. (e) Sun, S.; Zeng, H. *J. Am. Chem. Soc.* **2002**, *124*, 8204. (f) Park, J.; An, K.; Hwang, Y.; Park, J.-G.; Noh, H.-J.; Kim, J.-Y.; Park, J.-H.; Hwang, N.-M.; Hyeon, T. *Nat. Mater.* **2004**, *3*, 891.

(2) For reviews on bioapplications of magnetic nanoparticles, see: (a) Kumar, C. S. S. R.; Hormes, J.; Leuschner, C. *Nanofabrication Towards Biomedical Applications*; Wiley-VCH: Weinheim, Germany, 2005. (b) Mornet, S.; Vasseur, S.; Grasset, F.; Duguet, E. *J. Mater. Chem.* **2004**, *14*, 2161. (c) Pankhurst, Q. A.; Connolly, J.; Jones, S. K.; Dobson, J. *J. Phys. D: Appl. Phys.* **2003**, *36*, R167.

(3) For recent examples on bioapplications of magnetic nanoparticles, see: (a) Weissleder, R.; Kelly, K.; Sun, E. Y.; Shtatland, T.; Josephson, L. *Nat. Biotechnol.* **2005**, *23*, 1418. (b) de Vries, I. J. M.; Lesterhuis, W. J.; Barentsz, J. O.; Verdijk, P.; van Krieken, J. H.; Boerman, O. C.; Oyern, W. J. G.; Bonenkamp, J. J.; Boezeman, J. B.; Adema, G. J.; Bulte, J. W. M.; Scheene, T. W. J.; Punt, C. J. A.; Heerschap, A.; Figdor, C. G. *Nat. Biotechnol.* **2005**, *23*, 1407. (c) Won, J.; Kim, M.; Yi, Y.-W.; Kim, Y. H.; Jung, N.; Kim, T. K. *Science* **2005**, *309*, 121. (d) Huh, Y.-M.; Jun, Y.-w.; Song, H.-T.; Kim, S.; Choi, J.-S.; Lee, J.-H.; Yoon, S.; Kim, K.-S.; Shin, J.-S.; Suh, J.-S.; Cheon, J. *J. Am. Chem. Soc.* **2005**, *127*, 12387.

(4) Lee, I. S.; Lee, N.; Park, J.; Kim, B. H.; Yi, Y.-W.; Kim, T.; Kim, T. K.; Lee, I. H.; Paik, S. R.; Hyeon, T. *J. Am. Chem. Soc.* **2006**, *128*, 10658.

(5) (a) Son, S. J.; Reichel, J.; He, B.; Schuchman, M.; Lee, S. B. *J. Am. Chem. Soc.* **2005**, *127*, 7316, and references therein. (b) He, B.; Son, S. J.; Lee, S. B. *Langmuir* **2006**, *22*, 8263.

(6) Mitchell, D. T.; Lee, S. B.; Trofin, L.; Li, N.; Nevanen, T. K.; Soderlund, H.; Martin, C. R. *J. Am. Chem. Soc.* **2002**, *124*, 11864.

(7) (a) Okamaoto, K.; Shook, C. J.; Bivona, L.; Lee, S. B.; English, D. S. *Nano Lett.* **2004**, *4*, 233. (b) Son, S. J.; Lee, S. B. *J. Am. Chem. Soc.* **2006**, *128*, 15974.

(8) (a) Son, S. J.; Bai, X.; Nan, A.; Ghandehari, H.; Lee, S. B. *J. Controlled Release* **2006**, *114*, 143. (b) Lee, S. B.; Mitchell, D. T.; Trofin, L.; Nevanen, T. K.; Soderlund, H.; Martin, C. R. *Science* **2002**, *296*, 2198.

10.1021/cm703674d CCC: $40.75
Published on Web 05/23/2008

MSNT) can therefore be an ideal candidate for multifunctional nanomaterials aimed toward biomedical applications, such as biochemical separation and biosensing.[9] We report the synthesis of **Au-MSNT** and its uses for biochemical binding for specific proteins. We found that **Au-MSNTs** are bound to proteins possessing cysteine groups.

Experimental Section

Materials. GST protein was purified from BL21(DE3)pLysS transformed with pGEX-4T-1 using glutathione-sepharose. Ubiquitin proteins were obtained from Sigma.

Characterization. Transmission electron microscopy (TEM) images were obtained with a JEOL JEM-2010 transmission electron microscope operating at 200 kV. High-resolution TEM characterizations were performed with FEI Technai G2 F30 Super-Twin transmission electron microscope operating at 300 kV. The scanning electron micrographs of the samples were taken with a field emission scanning electron microscope (FE-SEM, FEI Sirion 400). Nitrogen-adsorption isotherms were measured at 78 K on a Micromeritics ASAP 2010 analyzer. The confocal microscope images were obtained using a LSM 510 Meta confocal microscope (from Zeiss) and a C-APOCHROMAT 63X/1.2w correction objective.

Synthesis of Cholesterol-Based Gelator 1. Cholesterol-based gelator **1**

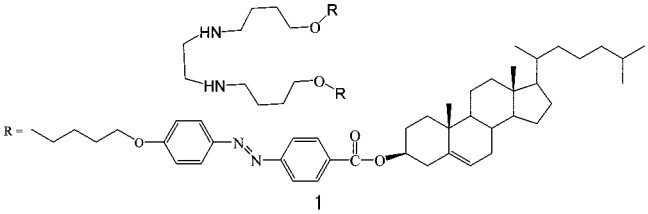

1

was synthesized as shown in Scheme S1 in the Supporting Information.

4-*n*-Monobromobutoxyl-4′-[(cholesteryloxy)carbonyl]azobenzene (3).[10] 4-[(Bromobutoxyphenyl)azo]benzoic acid **2** (0.7 g, 1.86 mmol) and cholesterol (0.718 g, 2.23 mmol) were dissolved in 20 mL of dichloromethane under a nitrogen atmosphere. The solution was maintained at 0 °C using an ice bath. The dicyclohexylcarbodiimide (DCC) (0.383 g, 1.86 mmol) and *N*,*N*-dimethylaminopyridine (DMAP) (0.022 g, 0.186 mmol) were then added, the reaction mixture being stirred for 4 h at 0 °C. The reaction mixture was filtered and the filtrate was washed with acidic and basic aqueous solutions (50 mL each). The organic layer was evaporated to dryness. The residue was purified by a silica-gel column eluting with THF/*n*-hexane (1:6 v/v) to give compound **6** in 26% yield as yellow solid (mp 141.5 °C). ^{1}H NMR: (300 MHz, $CDCl_3$) δ_H 8.17 (2H, d, $J = 9.0$), 7.72 (2H, d, $J = 9.0$), 7.90 (2H, d, $J = 9.0$), 7.10 (2H, d, $J = 9.0$), 5.45 (1H, d, $J = 6.3$), 5.02−4.88 (1H, m), 41 (2H, t, $J = 6.3$), 3.52 (2H, t, $J = 6.2$), 2.49 (2H, d, $J = 6.2$), 2.28−0.94 (35H, m), 0.88 (3H, s); (75 MHz, $CDCl_3$) δ_c 165.1, 161.88, 155.20, 146.98, 139.9, 130.2, 125.18, 122.84, 122.28, 114.72, 67.22, 66.67, 56.67, 56.11, 50.01, 42.30, 39.71, 39.50, 38.20, 37.01, 36.64, 36.17, 35.79, 33.32, 31.92, 31.86, 29.3, 28.32, 28.01, 27.88, 27.78, 24.28, 23.82, 22.83, 22.56, 21.04, 19.38, 19.38, 18.71, 11.86. MS(m/z) = 745 $[M + H]^+$. IR (KBr, υ_{max}/cm^{-1}): 3005 (Ar), 2935 (−CH), 1722 (−C═O), 1603, 1579, 1500, 1468 (Ar), 1284, 1116, 1047 (−C−O). Anal. Calcd for $C_{44}H_{61}N_2O_3Br$: C, 70.85; H, 8.24; N, 3.76. Found: C, 71.02; H, 8.25; N, 3.68.

4-(2-Ethyldiamino)butoxy-4′-bis[(cholesteyloxy)carbonylazobenzene] (1).[10] A mixture of compound **3** (0.1 g, 0.14 mmol), 1,2-diaminoethane (0.04 g, 0.67 mmol), and sodium carbonate (0.3 g, 6.7 mmol) in dry butyronitrile (10 mL) was refluxed for 24 h. The solution was filtered after cooling, the filtrate being concentrated to dryness by a vacuum evaporator. The residue was purified by an aluminum oxide column with ethanol/dichloromethane to give the desired product in 43.3% yield as yellow solid. ^{1}H NMR: (300 MHz, $CDCl_3$) δ_H 8.17 (4H, d, $J = 9.1$), 7.93 (4H, d, $J = 9.1$), 7.85 (4H, d, $J = 9.0$), 7.02 (4H, d, $J = 9.0$), 5.42 (2H, d, $J = 6.5$), 4.0−3.5 (6H, m), 3.0−0.9 (104H, m). MS (m/z) = 1392 $[M + 2H]^+$. IR (KBr, υ_{max}/cm^{-1}): 3005 (Ar), 2943 (−CH), 2868, 1715 (−C═O), 1595, 1582, 1500, 1468, 1419 (Ar), 1404, 1275, 1140, 1109 (−C−O). Anal. Calcd for $C_{90}H_{128}N_6O_6$: C, 77.77; H, 9.28; N, 6.05. Found: C, 75.52; H, 9.45; N, 6.15.

Preparation of MSNT. The cholesterol-based gelator **1** (45 mg) was added to acetic acid (900 mg) and warmed until the solution became transparent. The reaction mixture was placed at room temperature under static conditions for 10 h. Nickel(II) acetate (70 mg) and acetic acid (320 mg) were then added to the resulting mixture and again warmed until a transparent solution was obtained. The reaction mixture was maintained at room temperature under static conditions for 24 h. TEOS (240 mg) and water (120 mg) were then added to the resulting mixture and again warmed until a transparent solution was obtained. The reaction mixture was maintained at room temperature under static conditions for 5 days. Finally, the cholesterol-based gelator was intensively removed with THF. The samples were sealed in a glass tube and left at 20 °C for a day. Subsequently, they were heated at 200 °C for 1.0 h, 500 °C for 2 h under a nitrogen atmosphere, and finally at 500 °C for 4.0 h under aerobic conditions. Then, this was followed by the addition of 1.5 equiv of ascorbic acid as a reducing agent to mineralize the Ni nanocrystals on the silica nanotube. The size of Ni nanoparticles was estimated by a manual method.

Preparation of MSNT with Immobilized Mercaptopropyltriethoxysilane. Mercaptopropyltriethoxysilane (125 mg) was dissolved in anhydrous toluene (5 mL). The mixture was stirred under nitrogen for 2 min. The **MSNT** (40 mg) was added as solid. The reaction mixture was refluxed and stirred for 24 h. The collected solid was washed copiously with THF to rinse away any surplus mercaptopropyltriethoxysilane and then dried under vacuum.

Preparation of Au Nanoparticles. Gold nanoparticle seeds were prepared according to the literature.[11] Typically, this involves preparation of a 20 mL aqueous solution containing 2.5×10^{-4} M $HAuCl_4$ and 2.5×10^{-4} M trisodium citrate. To this solution was added 0.6 mL of ice cold 0.1 M $NaBH_4$ with stirring. The solution immediately turned orange-red, indicating formation of gold nanoparticles. The average particle size measured from transmission electron microscopy (TEM) was ∼2.0 nm. Citrate serves as a capping agent in this case, and gold particles are stable for a couple of weeks. To the vial was added 9.0 mL of growth solution containing a mixture of 2.5×10^{-4} M $HAuCl_4$ and 0.10 M CTAB solutions. To this solution was added 50 μL of 0.10 M freshly prepared ascorbic acid, and the resulting solutions were stirred gently. Next, 1.0 mL of the seed solution was mixed with vial solution. After 10 s, 1.0 mL was drawn from vial solution.

Preparation of Au-MSNT. To immobilize gold nanoparticles onto the surface of **MSNT**, the **MSNT** was added to Au nanopar-

(9) (a) Vemula, P. K.; Aslam, U.; Mallia, V. A.; John, G. *Chem. Mater.* **2007**, *19*, 138. (b) John, G.; Mason, M.; Ajayan, P. M.; Dordick, J. S. *J. Am. Chem. Soc.* **2004**, *126*, 15012. (c) Yang, W.-Y.; Ahn, J.-H.; Yoo, Y.-S.; Oh, N.-K.; Lee, M. *Nat. Mater.* **2005**, *4*, 399.

(10) (a) Jung, J. H.; Shinkai, S.; Shimizu, T. *Chem. Mater.* **2003**, *15*, 2141. (b) Jung, J. H.; Rim, J. A.; Lee, S. J.; Lee, S. S. *Chem. Commun.* **2005**, 468.

(11) Gearheart, N R.; Murphy Jana, L. C. J. *J. Phys. Chem. B* **2001**, *105*, 4065.

Scheme 1. Overall Scheme for the Synthesis of the Gold-Doped Silica Nanotube Obtained from Sol−Gel Transcription[a]

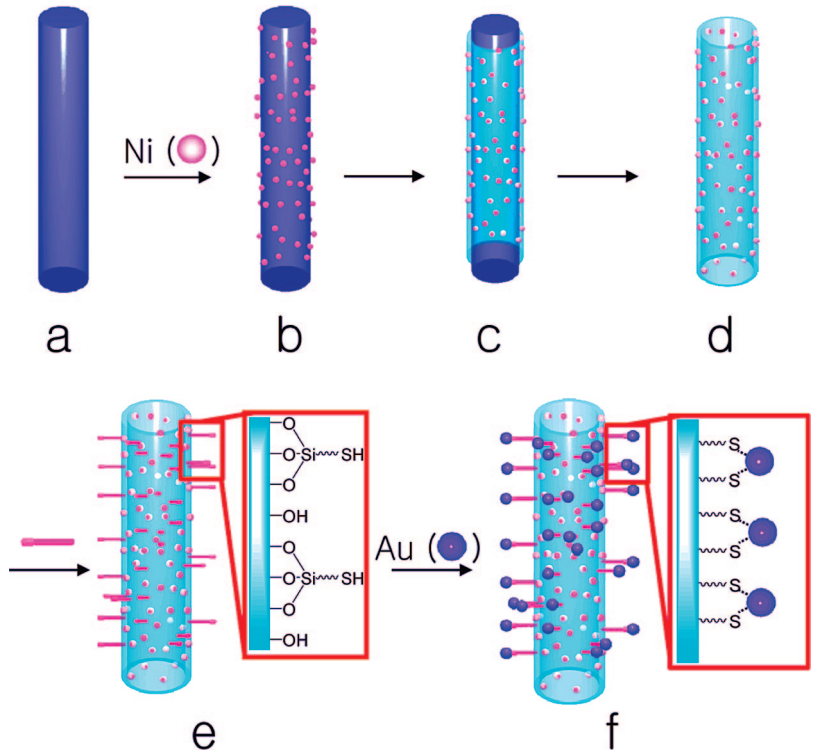

[a] (a) The self-assembled organogel fiber **1**, (b) organogel fiber complex formation with Ni (II) ion, (c) sol−gel polymerization of TEOS, (d) magnetic silica nanotube (**MSNT**) after calcination and reduction of Ni (II) with ascorbic acid, (e) **MSNT** with immobilized mercaptopropyltriethoxysilane, and (f) the gold-doped silica nanotube (**Au-MSNT**).

ticle solution (0.5 mL) for 24 h at room temperature. The collected solid was washed copiously with water (20 mL) four times to rinse away any surplus Au nanoparticles and then dried under vacuum.

Binding of Cysteine-Containing Proteins with Au-MSNT. The phosphate buffer solution (PBS/NaCl, KCl, Na_2HPO_4, KH_2PO_4, 200 μL) contains cysteine-containing proteins with added **Au-MSNT** (5 mg). The mixture was stirred at 0 °C in a darkroom for 1 day. The collected solid was washed copiously with water (10 mL) to rinse away any surplus cysteine-containing proteins.

Immunofluorescence Analysis. The **Au-MSNT** containing GST and ubiquitin protein were washed with 20 mM Tris-HCl, 150 mM NaCl, including 0.05% Tween20, pH 8.0 (TBST). The **Au-MSNT** was collected at low-speed centrifugation, 1000 rpm for 30 s. **Au-MSNT** was blocked with 5% nonfat dry milk. Tubes were incubated with primary antibodies as follows: mouse anti-GST antibody at a final concentration of 1 μg/mL (from Zymed); mouse anti-HA antibody at final concentration of 1 μg/mL (from Santa Cruz). Tubes were washed with TBST. A fluorescent secondary antibody (1:500, Alexa Fluor 488 goat antimouse IgG from Invitrogen) was used. The **Au-MSNT** was mounted in viscous solution (from Southern Biotech) on cell incubation coverslips. Pictures were taken using a LSM 510 Meta confocal microscope (from Zeiss) and a C-APOCHROMAT 63X/1.2w correction objective.

Results and Discussion

The methodology is outlined in Scheme 1.[12] First, the cholesterol-based gelator **1** in the presence of Ni(II) ion formed the fiber structure with ~220 nm diameter and several micrometer lengths. Second, oligomeric silica species are adsorbed onto the surface of the fibrous structure of gel **1** by electrostatic interaction and the polymerization further proceeds along these fibrils. This propagation mode eventually yields the tubular structure with a hollow cavity after calcination. Finally, 1.5 equiv of ascorbic acid as a reducing agent to mineralize the Ni nanocrystals was added to the silica nanotube (see Experimental Section for details).

Following the modification of the surface of **MSNT** with mercaptopropyltriethoxysilane, the **MSNT** was added to a solution of 500 μL of 2 nm Au nanoparticles and incubated at 25 °C for 20 h. Excess Au nanoparticles remaining in solution were removed by filtration and washed with water four times. Finally, Au-doped **MSNT** was characterized by scanning electron microscopy (SEM), transmission electron microscopy (TEM), energy-dispersive X-ray (EDX), and FT-IR.

Figure 1a−c shows the SEM and TEM images of nickel-doped magnetic silica nanotube (**MSNT**). The nickel nanoparticles with 3.5 ± 1.0 nm are homogeneously deposited on the inner side of **SNT** with 220 nm diameter. Figure 1d shows the room-temperature magnetization curve of **MSNT** obtained by a superconducting quantum interference device (SQUID). The **MSNT** exhibits superparamagnetic characteristics. This saturation magnetization is 0.1052 emu/g at 300 K. Furthermore, the deposition of nickel nanoparticles in the **SNT** was confirmed by EDX (Figure S1), field emission scanning electron microscopy (FE-SEM), and high-

(12) (a) Jung, J. H.; Ono, Y.; Hanabusa, K.; Shinkai, S. *J. Am. Chem. Soc.* **2000**, *122*, 5008. (b) Jung, J. H.; Ono, Y.; Shinkai, S. *Angew. Chem., Int. Ed* **2000**, *39*, 1862.

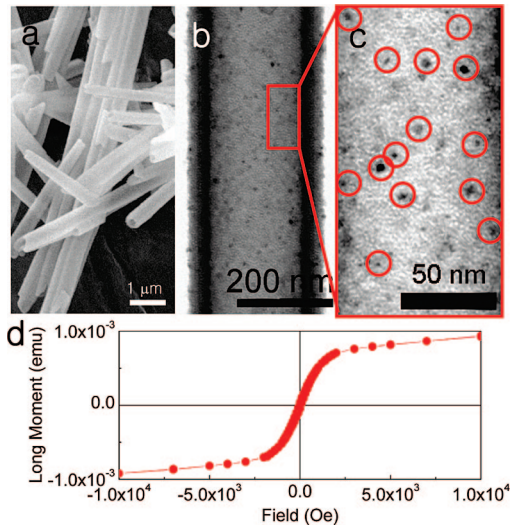

Figure 1. (a) SEM image and (b and c) TEM images of **MSNT**. (d) An hysteresis loop showing superparamagnetic properties of **MSNT** at room temperature. Cycles indicate Ni nanoparticles.

resolution TEM (HRTEM) (Figure S2). The electron diffraction pattern of a high-resolution TEM image of a single particle revealed an atomic lattice fringe with a 0.28 nm distance for (111) (Figure S2).

To generate attachment sites for Au nanoparticles on the surface of **MSNT**, **MSNT** was added to a solution of mercaptopropyltriethoxysilane in toluene. The mixture was refluxed for 24 h and filtered. After drying, the product was evaluated by TEM, EDX, BET isotherm analysis, and FT-IR (Figures S3−S6). EDX measurement confirmed the presence of sulfur atoms. Furthermore, the surface area of **MSNT** with immobilized mercaptopropyltriethoxysilane was 119 m^3/g, much smaller than the surface area prior to mercaptopropyltriethoxysilane modification (Figure S5). This means that the mercaptopropyltriethoxysilane group was immobilized onto the surface of the **MSNT**.[13] Also, after attachment of mercaptopropyl-triethoxysilane in **MSNT**, the CH_2 stretching peak appeared at 2900 cm^{-1} in the FT-IR spectrum (Figure S6), strongly indicating the covalent attachment of the mercaptopropyltriethoxysilane group onto the surface of **MSNT**. In addition, **MSNT** was examined independently by elemental mapping with electron energy-loss spectroscopy (Figure S7). The material (Figure S7, a) contains silicon (Figure S7, b), oxygen (Figure S7, c), nickel (Figure S7, d), sulfur (Figure S7, e), and carbon (Figure S7, f) components. The distribution of Ni nanoparticles and sulfur component shows a one-dimensional structure (Figure S7, d and e), strongly implying that Ni and sulfur atom were homogeneously deposited onto the surface of the **MSNT**.

Immobilization of gold nanoparticles onto the surface of the **MSNT** was verified by TEM (Figure 2A). The TEM image clearly revealed the Au nanoparticles with 9.3 ± 2.0 nm diameter. In addition, the electron diffraction pattern of a high-resolution TEM image of a single particle revealed an atomic lattice fringe with a 0.23 nm distance for (111)

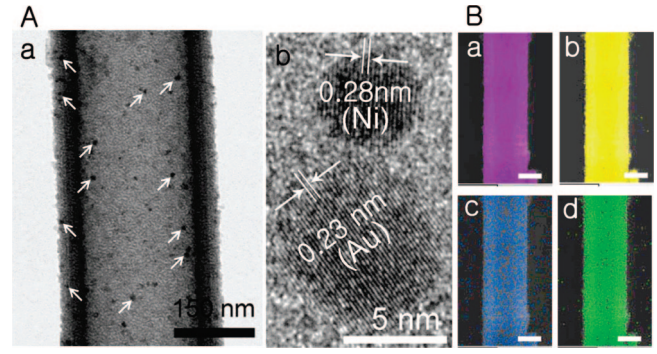

Figure 2. (A): (a) TEM and (b) high-resolution TEM images of **Au-MSNT**. (B): Elemental mapping of **Au-MSNT** by electron energy-loss spectroscopy (EELS): (a) Si component, (b) O component, (c) Ni component, and (d) Au component. Arrows indicate Ni and Au nanparticles. Scale bar (B): 100 nm.

(Figure 2A, b), which is consistent with a face-centered cubic (fcc) crystalline structure.

Furthermore, Au-doped **MSNT** (**Au-MSNT**) was examined independently by elemental mapping with electron energy-loss spectroscopy (Figure 2B). The material contains silicon (Figure 2B, a), oxygen (Figure 2B, b), nickel (Figure 2B, c), and gold (Figure 2B, d) components. The distribution of Au nanoparticles shows a one-dimensional structure (Figure 2B, d), strongly implying again that Au nanoparticles associated with sulfur atom were homogeneously deposited onto the surface of the **MSNT**.

For a definitive biomolecular recognition experiment, **Au-MSNT** was added to an aqueous phosphate buffer solution, pH 7, of glutathione S-transferase (GST), a protein possessing cysteine groups. The excess protein remaining in solution was removed by magentic separation and the **Au-MSNT** was washed with water. We observed the selective binding of protein onto the surface of **Au-MSNT** by confocal microscopy. GST is a protein containing four cysteine residues, with one cysteine on its surface pocket area.[14] GST proteins bound to the surface of **Au-MSNT** were detected by an immunofluorescence method (Figure 3A). Anti-GST antibodies could bind to GST on the surface of **Au-MSNT** specifically. Fluorescent secondary antibodies could bind to anti-GST primary antibodies on the surface (Figure 3A). It means that GST proteins exist on the surface as stable bound forms. Once again, the thiol groups of GST proteins are stably bound to Au nanoparticles deposited onto the silica nanotubes by covalent bond.[15] The specificity of the interaction between **Au-MSNT** and cysteine was demonstrated by studies with ubiquitin, a protein lacking cysteine, which could not bind to **Au-MSNT** (Figure 3B). Nonspecific fluorescent secondary antibody binding to **Au-MSNT** was negligible (Figure 3B). These results indicate that **Au-MSNT** may be useful as a biosensor to detect cysteine-containing proteins.

In this study, probably the main driving force of protein binding to the surface of **Au-MSNT** is specific interaction, but not nonspecific interaction. Thus, the sulfur atoms of GST are bound to the Au nanoparticles on the surface of **Au-MSNT** by covalent bond. On the other hand, the ubiquitin

(13) (a) Lee, S. J.; Lee, J.-E.; Seo, J.; Jeong, I. Y.; Lee, S. L.; Jung, J. H. *Adv. Funct. Mater* **2007**, *17*, 3441. (b) Lee, S. J.; Lee, S. S.; Hong, J. M.; Lah, M. S.; Jung, J. H. *Chem. Commn.* **2006**, 4539.

(14) McTigue, M. A.; Williams, D. R.; Tainer, J. A. *J. Mol. Biol.* **1995**, *246*, 21.

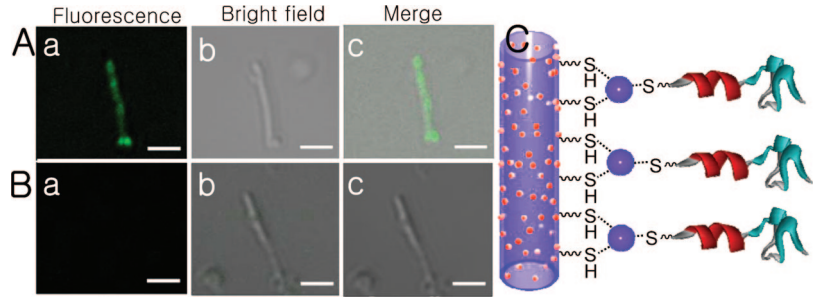

Figure 3. Confocal images of **Au-MSNT** with (A) GST by treatment of anti-GST antibody and (B) ubiquitin by treatment of antiubiquitin antibody: (a) fluorescence, (b) bright field, and (c) merge images. (C). Illustration for binding mode of **Au-MSNT** with GST protein. Scale bar: 2 μm.

did not bind to thesurface of **Au-MSNT** due to the lack of cysteine groups.

To prove the specific interaction between Au nanoparticles and thiol group, GST was added to **MSNT** to confirm the role of Au nanoparticles. As shown in Figure S8, we could not observe fluorescent emission from the **MSNT**, indicating that anti-GST antibodies did not bind to the **MSNT**. In the present case, we believe that the weakly bound proteins on the **MSNT** are completely removed by the washing process with TBST (20 mM Tris-Cl, 150 mM NaCl, 0.05% Tween-20, pH 8.0) solution and hence the **MSNT** does not show any fluorescence under confocal microscopic observation.

Furthermore, ubiqutin used as a control protein possesses methionine moiety, which contains sulfur as a form of methyl sulfur ($-SCH_3$). However, in control experiment, **Au-MSNT** in an immonofluorescence binding assay did not bind to ubiqutin protein. The reason why **Au-MSNT** can not bind to the sulfur of methionine might be that the methyl group (CH_3S-) of methionine blocks interaction between sulfur and gold of **Au-MSNT** and/or methionine group exists in the inside of the three-dimensional structure of ubiqutin protein. This finding indicates that **Au-MSNT** is useful as a receptor for the protein possessing cysteine group.

Conclusions

We demonstrated the synthesis of **Au-MSNT** and its successful application to binding of cysteine-containing proteins. On the other hand, ubiquitin, which has no cysteine groups, was not immobilized onto the **Au-MSNT**. These results indicate that the **Au-MSNT** is efficiently recognized by the cysteine-containing protein. Such **Au-MSNT** holds much promise as candidates for various applications, including chemical and biochemical separations. We believe that our approach can be employed to anchor biomolecules onto nanostructures, thereby producing novel biomedical nanomaterials.

Acknowledgment. This work was supported by the Korea Research Foundation Grant (KRF-2005-070-C00068 and KRF-2005-070-C00089) and KOSEF (R01-2007-000-20229-0 and National Honor Scientist Program: 2006-05106).

Supporting Information Available: TEM images, EDX spectrum, nitrogen adsorption−desorption isotherms, FT-IR spectrum, and elemental mapping of **MSNT** (PDF). This materials is available free of charge via the Internet at http://pubs.acs.org.

CM703674D

(15) (a) Shang, L.; Qin, C.; Wang, T.; Wang, M.; Wang, L.; Dong, S. *J. Phys. Chem. C* **2007**, *111*, 13414. (b) Shimada, T.; Ookubo, K.; Komuro, N.; Shimizu, T.; Uehara, N. *Langmuir* **2007**, *23*, 11225. (c) Kou, X.; Zhang, S.; Yang, Z.; Tsung, C.-K.; Stucky, G. D.; Sun, L.; Wang, J.; Yan, C. *J. Am. Chem. Soc.* **2007**, *129*, 6402.